

Anatomy of One-Dimensional Cocrystals: Randomness into Order

Seokhoon Ahn and Adam J. Matzger*

Department of Chemistry and the Macromolecular Science and Engineering Program, University of Michigan, Ann Arbor, Michigan 48109-1055

Received July 1, 2009; E-mail: matzger@umich.edu

Abstract: A 2D cocrystal that displays random mixing along one axis and periodic ordering along the other axis is discovered. The characteristics and formation process of this “1D-cocrystal” are examined with atomic detail by scanning tunneling microscopy (STM) at the liquid/solid interface and through computed models. This type of cocrystallization causes an alignment shift to satisfy close packing. The frequency of the alignment shift can be controlled by variation of the ratio of adsorbates in solution. Furthermore, a reversible monolayer reorganization induced through perturbing the STM bias voltage provides not only mechanistic insights into the formation process of the 1D-cocrystal but also the potential for applications as a molecular switch. The control over surface composition and periodicity by controlling the molar ratio of components offers an unexploited approach to nanoscale patterning.

Introduction

Most crystallizations conducted in contexts from the laboratory to industrial production involve multicomponent solutions yielding one or more phases. Because of the importance of such processes in purification and solid form engineering, the outcomes of these crystallizations have been studied in great detail with classification schemes describing three general outcomes: (1) segregated single component phases, (2) a homogeneous phase of stoichiometric composition (cocrystallization), and (3) a solid solution. In two-dimensional (2D) crystallizations these same issues arise and the outcome is particularly important for understanding the composition and structure of adsorbed molecules at liquid/solid interfaces. Searching the Two-Dimensional Structural Database (2DSD),¹ a catalog of packing patterns for molecules adsorbed at the liquid/solid interface, reveals that, with some notable exceptions related to the emergence of chirality, the similarities between crystallization in two and three dimensions are quite striking with phase segregation, random mixing, and cocrystallization observed commonly in the 2DSD. An advantage of studying this reduced dimensionality system when endeavoring to understand crystallization from multicomponent solutions is that phases which are not fully periodic, and therefore not well suited to study by diffraction techniques, can readily be imaged in a time dependent fashion using scanning tunneling microscopy (STM) offering structural and mechanistic insights.²

A multicomponent solution in contact with highly oriented pyrolytic graphite (HOPG) can lead to coadsorption. This may manifest as phase segregation,³ random mixing⁴ or cocrystallization.⁵ In general, phase segregation occurs when each component adopts a structure that is identical to that obtained from pure solution. For example, *n*-tetracontane (C₄₀H₈₂) and 4'-octyl-4-biphenylcarbonitrile (8CB) grow crystals in distinct domains due to the different size of the molecules and incompatibility between functional groups.³ Random mixing occurs when one component is incorporated into the structure of another in a nonperiodic fashion. For example, hexadecyl sulfide ((CH₃(CH₂)₁₅)₂S) inserts randomly into the self-assembled monolayer of tritriacontane (C₃₃H₆₈) without disruption of the original monolayer structure because these molecules are of similar dimensions.^{4a} This phenomenon is observed when two species have sufficiently similar size and functionality to be compatible. Cocrystallization commonly occurs in two situations: (1) strong intermolecular interaction of two different molecules to form an ordered periodic structure such as adenine-thymine (A-T)^{5c} and guanine-uracil (G-U)^{5d} base pairs by hydrogen bonding and (2) filling empty space in an open lattice,

(1) Plass, K. E.; Grzesiak, A. L.; Matzger, A. J. *Acc. Chem. Res.* **2007**, *40*, 287–293.

(2) (a) Li, S. S.; Yan, H. J.; Wan, L. J.; Yang, H. B.; Northrop, B. H.; Stang, P. J. *J. Am. Chem. Soc.* **2007**, *129*, 9268–9269. (b) Lei, S.; Tahara, K.; Feng, X.; Furukawa, S.; De Schryver, F. C.; Müllen, K.; Tobe, Y.; De Feyter, S. *J. Am. Chem. Soc.* **2008**, *130*, 7119–7129. (c) Scherer, L. J.; Merz, L.; Constable, E. C.; Housecroft, C. E.; Neuburger, M.; Hermann, B. A. *J. Am. Chem. Soc.* **2005**, *127*, 4033–4041. (d) Fang, H.; Giancarlo, L. C.; Flynn, G. W. *J. Phys. Chem. B* **1999**, *103*, 5712–5715.

(3) Baker, R. T.; Mougous, J. D.; Brackley, A.; Patrick, D. L. *Langmuir* **1999**, *15*, 4884–4891.

(4) (a) Padowitz, D. F.; Messmore, B. W. *J. Phys. Chem. B* **2000**, *104*, 9943–9946. (b) Xie, Z. X.; Xu, X.; Mao, B. W.; Tanaka, K. *Langmuir* **2002**, *18*, 3113–3116.

(5) (a) Tao, F.; Bernasek, S. L. *J. Am. Chem. Soc.* **2005**, *127*, 12750–12751. (b) Yang, X.; Mu, Z.; Wang, Z.; Zhang, X.; Wang, J.; Wang, Y. *Langmuir* **2005**, *21*, 7225–7229. (c) Mamdough, W.; Dong, M.; Xu, S.; Rauls, E.; Besenbacher, F. *J. Am. Chem. Soc.* **2006**, *128*, 13305–13311. (d) Mamdough, W.; Kelly, R. E. A.; Dong, M.; Kantorovich, L. N.; Besenbacher, F. *J. Am. Chem. Soc.* **2008**, *130*, 695–702. (e) Kampschulte, L.; Werblowsky, T. L.; Kishore, R. S. K.; Schmittl, M.; Heckl, W. M.; Lackinger, M. *J. Am. Chem. Soc.* **2008**, *130*, 8502–8507. (f) Schull, G.; Douillard, L.; Fiorini-Debuisschert, C.; Charra, F.; Mathevet, F.; Kreher, D.; Attias, A.-J. *Nano Lett.* **2006**, *6*, 1360–1363. (g) Furukawa, S.; Tahara, K.; De Schryver, F. C.; Auweraer, M. V.; Tobe, Y.; De Feyter, S. *Angew. Chem., Int. Ed.* **2007**, *46*, 2831–2834.

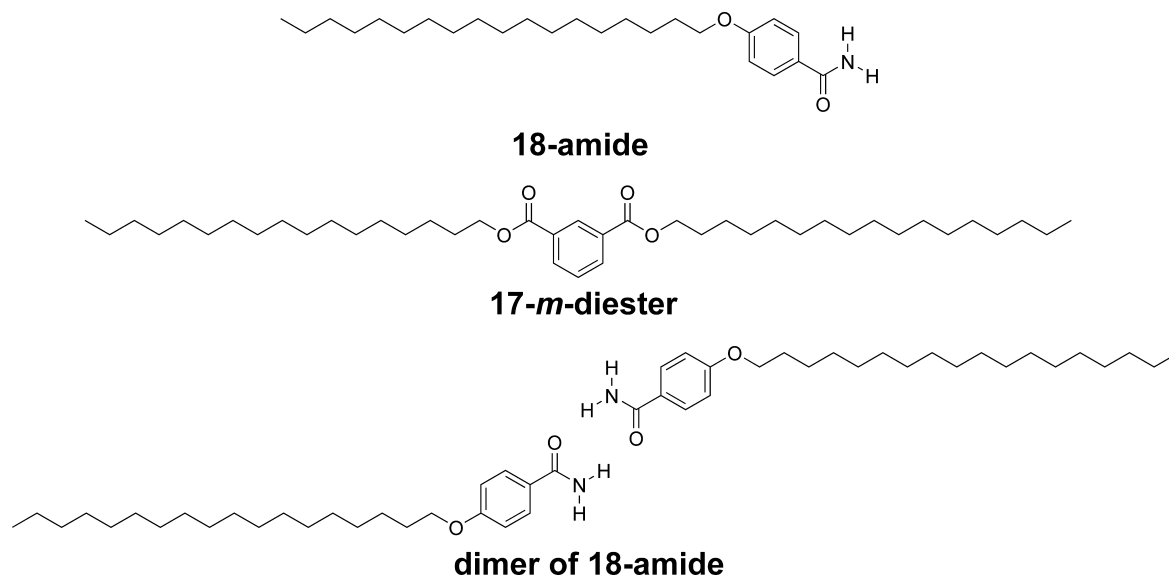


Figure 1. Chemical structures of molecules imaged by STM.

such as incorporation of coronene into the open structure formed by a star-shaped stilbenoid compound,^{5f} (host–guest behavior) or in cases where close packing is not well satisfied in a single component structure.⁶

During studies of the competitive adsorption of two components at the liquid/solid interface, we observed a new type of cocrystal, distinguished from the three general outcomes described above. This supramolecular assembly has characteristics of both random mixing and traditional cocrystals. Because this cocrystal shows not only periodicity along one axis but also nonperiodicity along the other axis, it is described as a one-dimensional (1D) cocrystal. This novel packing pattern was characterized by high resolution STM imaging complemented by computed models, and the formation process was examined through temporally resolved imaging of reversible monolayer reorganization induced by perturbing the STM bias voltage; such composition changes hold potential for applications in high density data storage based on information coding with molecular-scale features.⁷ Finally, to define this novel cocrystallization behavior, the types of 2D crystallization obtained from the multicomponent systems were analyzed in the 2DSD.

Results and Discussion

Chemical structures of the compounds employed in 2D crystallization are shown in Figure 1. The competitive adsorption of 4-octadecyloxybenzamide (**18-amide**) and diheptadecyl isophthalate (**17-m-diester**) at the 1-phenyloctane/graphite interface was monitored by STM under ambient conditions. The size and shape of molecules and the compatibility of their functional groups play a key role in determining crystallization behaviors such as phase segregation and random mixing; from these criteria, phase segregation of **18-amide** and **17-m-diester**

was expected due to the dissimilar size/shape and lack of complementary functionality. Although dimerization of the **18-amide** is likely to occur in phenyloctane solution, this unit is still sufficiently different in size and shape from **17-m-diester** that random mixing would not be predicted. Against these expectations, the observed behavior, that in several aspects more closely resembles random mixing, is intriguing and derives from a subtle compatibility between the conformation of the self-assembled **17-m-diester** and the dimer structure of **18-amide**. This mechanism is discussed below in the context of the formation process of a 1D-cocrystal.

Characteristics of 1D-Cocrystal. The phases of pure **17-m-diester** have been reported previously.⁸ In the lowest energy packing, the column of benzene rings of **17-m-diester** is aligned perpendicular to the alkyl chains and these alkyl chains are interdigitated to give a close-packed structure in the plane group *cm* (Figure 2a). The phase of pure **18-amide** in phenyloctane is characterized by noninterdigitated alkyl chains with amides participating in a hydrogen bonding network (see Supporting Information).⁹ When a mixture of **17-m-diester** and **18-amide** is present in solution, however, insertion of **18-amide** into the **17-m-diester** monolayer occurs as evidenced by the appearance of bright elongated spots corresponding to the aromatic part of the inserted dimer (Figure 2b). These coadsorbed dimers of **18-amide** are arranged in lines that extend infinitely; the spacing between these lines is not regular and this nonperiodic lattice direction is designated as the nonperiodic axis (NPA). A second axis, where molecular composition repeats at defined intervals with a characteristic length scale, is termed the periodic axis (designated PA). The arrangement of the two components results in an unusual unit cell which is represented as white lines in Figure 2b. The width of the unit cell, *a*, is 6.10 nm which corresponds closely to the computed dimer length of 6.05 nm. The other parameter of the unit cell is infinite due to the nonperiodicity. Because this infinite unit cell is only repeated along the PA, this type of 2D crystal is best termed a 1D-cocrystal.

(6) For discussion of this phenomenon in three dimensional crystals structures, see: Price, C. P.; Glick, G. D.; Matzger, A. J. *Angew. Chem., Int. Ed.* **2006**, *45*, 2062–2066.

(7) (a) Cavallini, M.; Biscarini, F.; Leon, S.; Zerbetto, F.; Bottari, G.; Leigh, D. A. *Science* **2003**, *299*, 531. (b) Feng, M.; Gao, L.; Deng, Z.; Ji, W.; Guo, X.; Du, S.; Shi, D.; Zhang, D.; Zhu, D.; Gao, H. *J. Am. Chem. Soc.* **2007**, *129*, 2204–2205. (c) Sato, A.; Tsukamoto, Y. *Adv. Mater.* **1994**, *6*, 79–80. (d) Shang, Y.; Wen, Y.; Li, S.; Du, S.; He, X.; Cai, L.; Li, Y.; Yang, L.; Gao, H.; Song, Y. *J. Am. Chem. Soc.* **2007**, *129*, 11674–11675.

(8) Plass, K. E.; Kim, K.; Matzger, A. J. *J. Am. Chem. Soc.* **2004**, *126*, 9042–9053.

(9) Ahn, S.; Morrison, C. N.; Matzger, A. J. *J. Am. Chem. Soc.* **2009**, *131*, 7946–7947.

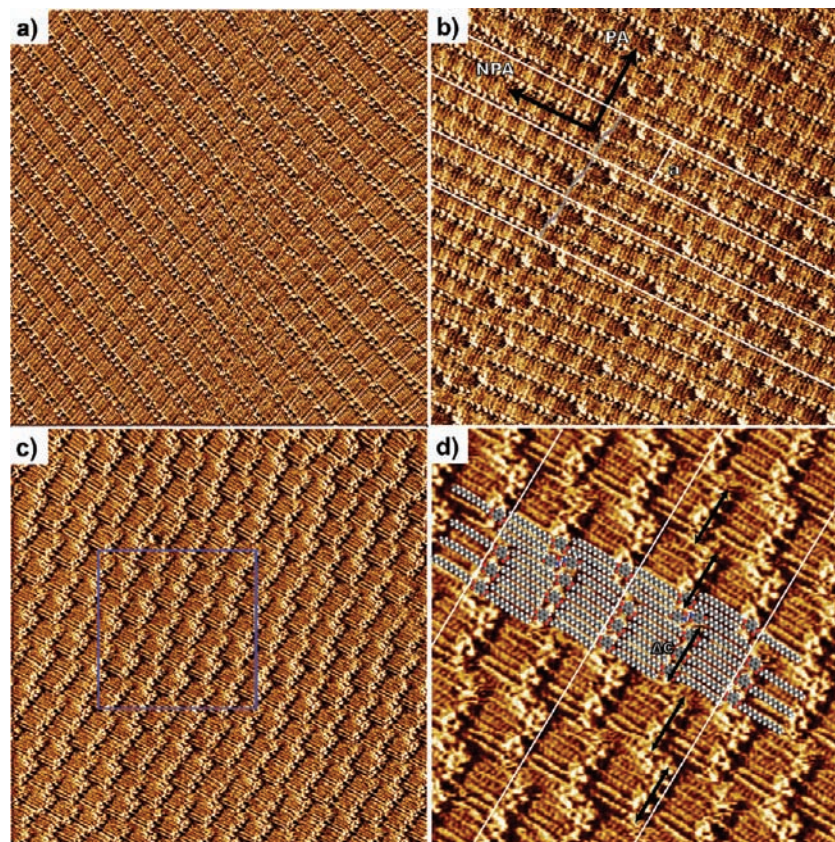


Figure 2. STM Images of (a) **17-*m*-diester** and (b) 1D-cocrystal formed by inserting dimers of **18-amide** into **17-*m*-diester** columns from a 20:1 mixture (**17-*m*-diester:18-amide**) in phenyloctane on HOPG ($50 \times 50 \text{ nm}^2$, 10.2 Hz, 800 mV, 300 pA). Black arrows indicate the periodic axis (PA) and the nonperiodic axis (NPA). (c) STM image of 1D-cocrystal from a 12:1 mixture (**17-*m*-diester:18-amide**) on HOPG ($50 \times 50 \text{ nm}^2$, 10.2 Hz, 800 mV, 300 pA). The blue square in (c) indicates a region where there is a saturation effect on column length. (d) Magnified STM image ($20 \times 20 \text{ nm}^2$) of the blue square area indicated in (c). An arrow represents a column length (ΔC) of contiguous **17-*m*-diester** molecules in each column. An optimized molecular model is overlaid to aid visualization of the molecular conformation and white lines represent unit cells of 1D-cocrystal (b,d).

The 1D-cocrystal is characterized by an alignment shift of **17-*m*-diester** columns through inserting **18-amide** molecules, and as the mole fraction of **18-amide** in solution increases the alignment shift happens with increased frequency due to more prevalent random mixing of **18-amide** (Figure 2c). Upon increasing the proportion of **18-amide** from 20:1 to 12:1 (**17-*m*-diester:18-amide**), there is a dramatic change from nonperiodicity to pseudoperiodicity along the NPA and an absence of pure phases of either **18-amide** or **17-*m*-diester**. Pseudoperiodicity describes this phenomenon because the spacing in the second dimension is almost regular; for example, one area of the 1D-cocrystal monolayer shows a periodic pattern indicated by a blue square in Figure 2c. Inspection of an expanded region of the 12:1 mixture offers detailed structural information (Figure 2d). In order to complement STM images, the computed model of the 2D crystal in this region was constructed based on high resolution images and energy minimized to obtain the optimized packing structure (Figure 3). The relative orientation of **17-*m*-diester** molecules on either side of the **18-amide** row can be determined by observing the relative brightness of the columns of aromatic rings; opposite orientations of C=O groups has been demonstrated to result in a slight variation in aromatic ring contrast.^{8,10} No contrast difference is observed in the present case suggesting that the orientation of **17-*m*-diester** is the same

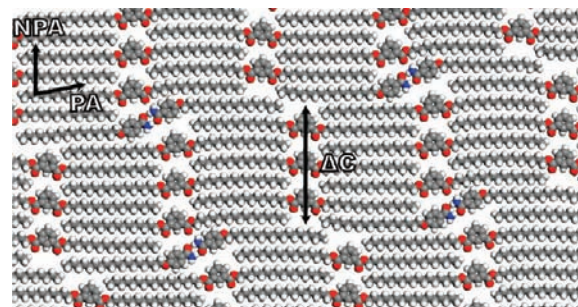


Figure 3. Computed packing pattern of 1D-cocrystal showing a repeat distance along the NPA at a 12:1 molar ratio (**17-*m*-diester:18-amide**). An arrow represents a column length (ΔC) of 3.00 nm of contiguous **17-*m*-diester** molecules in each column.

on both sides of the **18-amide** row. The symbol ΔC in Figure 3 represents the column length of contiguous **17-*m*-diester** molecules in each column. The experimental value for ΔC corresponding to three inserted molecules is 3.12 nm and this value matches well with the ΔC of 3.00 nm from the computed model.

Further increasing the proportion of **18-amide** from the 12:1 mixture does not lead to more insertion of **18-amide** into the 1D-cocrystal. To explore the origin of this saturation effect, lattice energies were computed for several observed and hypothetical packing patterns normalized to a per unit cell area

(10) De feyter, S.; Grim, P. C. M.; van Esch, J.; Kellogg, R. M.; Feringa, B. L.; De Schryver, F. C. *J. Phys. Chem. B* **1998**, *102*, 8981–8987.

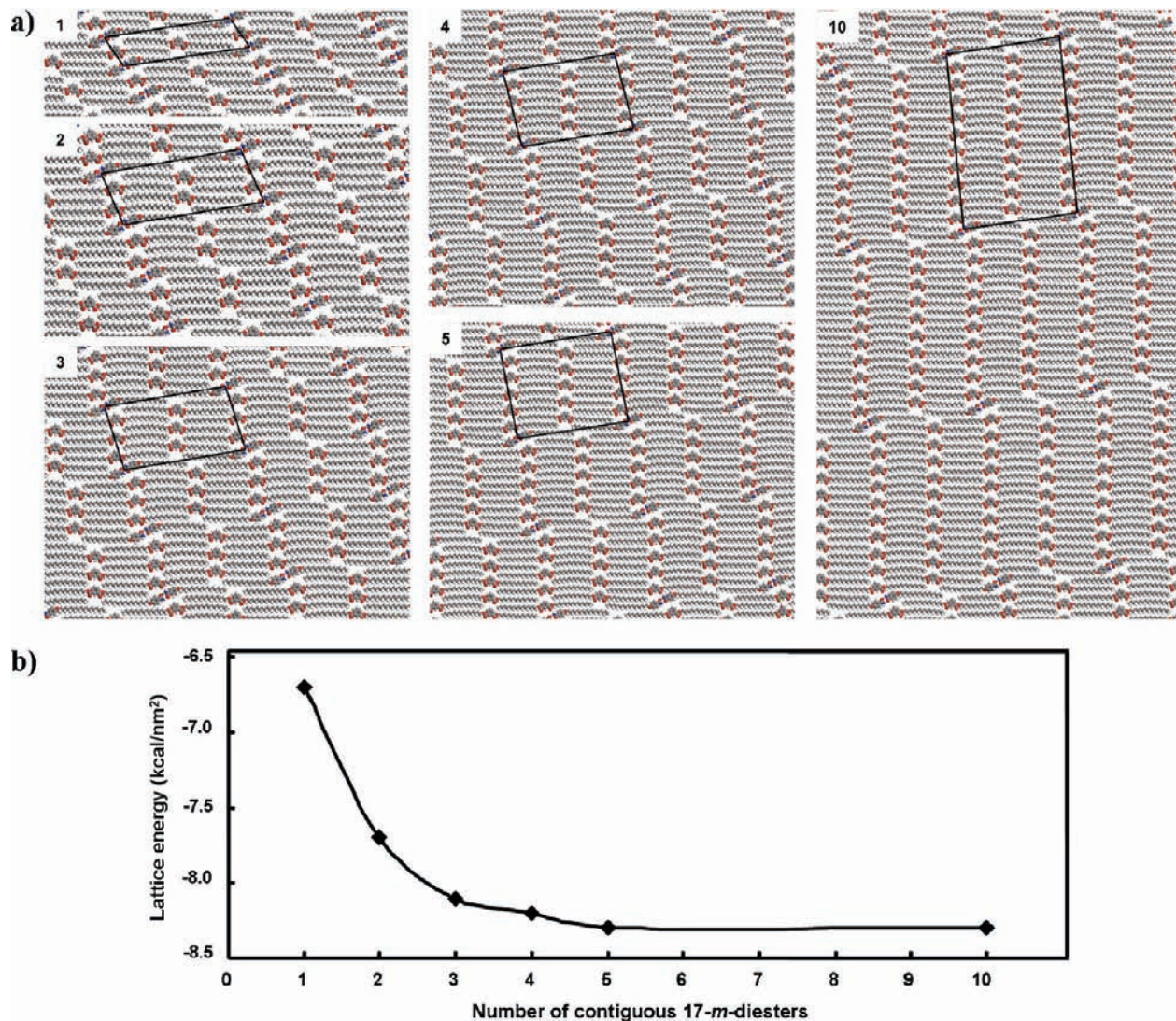


Figure 4. (a) Periodic models of 1D-cocrystals depending on the column length of contiguous **17-m-diester** molecules in each column. The inset value indicates the numbers of these contiguous **17-m-diester** molecules. (b) Lattice energies computed by the COMPASS force field (kcal/nm²) based on the periodic 1D-cocrystal models. The values represent the energy obtained by the formation of the periodic assembly from isolated **17-m-diester** and the dimer of **18-amide**.

basis.¹¹ These energies were obtained by constructing fully periodic 1D-cocrystals with various ΔC (Figure 4a).¹² The change in lattice energy is small as ΔC decreases from 10 to 3. However, when the column length is shorter than 3, the lattice energy of the 2D crystals becomes dramatically less negative due primarily to a significant reduction in van der Waals interactions. The contribution to the lattice energy from the

electrostatic term is uniformly small because the **17-m-diester** phase is primarily stabilized through alkyl chain interdigitation (see Supporting Information). Experimentally, the average ΔC changes from 10.86 to 3.61 nm as the proportion of **18-amide** increases from 20:1 to 12:1 (**17-m-diester**:**18-amide**) and the fact that substantially smaller ΔC values are not obtained agrees well with the computations and leads to the observed saturation behavior. These results reveal that surface composition can be controlled by variation of the ratio of adsorbates in solution so that nanoscale features arise from the alignment shift, offering a facile approach to 2D patterning. Notably, this structural modulation occurs perpendicular to the long molecular axis: the most difficult direction to control nanoprecision in these types of physisorbed monolayers.¹³

Formation Process. The formation of the 1D-cocrystal is proposed to arise through a mechanism having characteristics of both random mixing and cocrystallization. During the

- (11) The stabilization energies on a per unit cell area basis have been discussed to compare the stability of 2D crystals (see: Kim, K.; Plass, K. E.; Matzger, A. J. *J. Am. Chem. Soc.* **2005**, *127*, 4879–4887.) because a per molecule basis could not be applied due to compositional changes in the monolayer.
- (12) (a) After energy minimization of each fully periodic 1D-cocrystal model, the energies of isolated molecules of **17-m-diester** and the dimer of **18-amide** are subtracted to get the stabilization energies per a unit cell. These values are divided by the area of each unit cell to get the stabilization energies on a per unit area. (b) As pointed out by one reviewer, the unit cells in Figure 4a contain $2n+1$ molecules, where n is the **17-m-diester** column length and the **18-amide** dimer is treated as a single unit. The number of defects (**18-amide** dimers) in these unit cells varies as $1/(2n+1)$. The plot in Figure 4 is well fit by Lattice energy = $6.71 \text{ kcal/nm}^2 \times (1/(2n+1)) - 8.94 \text{ kcal/nm}^2$. The density of defects is determined by a 6.71 kcal/nm^2 energy increase.

- (13) (a) Wei, Y.; Tong, W.; Zimmt, M. B. *J. Am. Chem. Soc.* **2008**, *130*, 3399–3405. (b) Plass, K. E.; Engle, K. M.; Cychosz, K. A.; Matzger, A. J. *Nano Lett.* **2006**, *6*, 1178–1183.

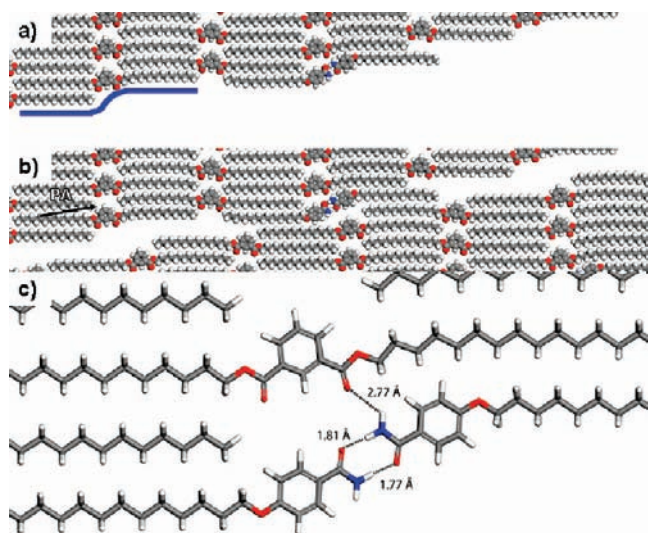


Figure 5. Suggested models for the 1D cocrystallization process. (a) Initial coadsorption model showing geometric and functional compatibility. A blue line shows the geometry of the domain edge of **17-*m*-diester** matches well with the shape of the dimer of **18-amide**. (b) Model with two dimers abstracted from the 1D cocrystal to illustrate the void space shape, and (c) the computed hydrogen bond distances of (a) showing compatibility of functionality.

adsorption of **17-*m*-diester**, the dimer of **18-amide** may interrupt this process; although the amide can not substitute directly in the lattice of the diester due to the size difference, the compatibility of shape and functionality between the **18-amide** dimer and the monolayer structure of **17-*m*-diester** (Figure 5a) allows insertion at the propagating front. The shape of the domain edge of **17-*m*-diester** is compatible with that of the dimer of **18-amide** (blue line in Figure 5a) and furthermore there is an attractive interaction between **17-*m*-diester** and **18-amide** mediated by hydrogen bonding (Figure 5c). The computed N–H...O distances of 1.81 and 1.77 Å between two **18-amide** molecules are well within the typical values of hydrogen bonding distances (1.6–2.0 Å). The computed N–H...O distance of 2.77 Å and angle of 141.7° between **17-*m*-diester** and **18-amide** indicates weak hydrogen bonding thus stabilizing the coadsorbed dimer of **18-amide**. Therefore, the combination of the compatibility of shape and functionality between the dimer of **18-amide** and the monolayer structure of **17-*m*-diester** results in random mixing along the NPA. After this random mixing, a new propagation of **17-*m*-diester** may start from the inserted dimer of **18-amide** and this causes the alignment shift of **17-*m*-diester** (Figure 5b). This shift is driven by close packing. Because there is no significant interaction such as hydrogen bonding between the dimer and the newly propagated **17-*m*-diester** molecule, the tendency for 2D crystals to satisfy close packing will determine the crystal structure.¹ This driving force makes it possible to shift the alignment of **17-*m*-diester**. This realignment of **17-*m*-diester** creates some space as shown in Figure 4b. At this point, one hypothesis is needed to explain 1D periodicity. The hypothesis is that filling this space with the dimer is thermodynamically more favorable than filling with **17-*m*-diester** because the dimer more effectively reduces void space. Based on this hypothesis, dimers of **18-amide** can be periodically aligned along the PA by satisfying close packing. Experimental verification of this hypothesis was obtained through reversible monolayer reorganization.

Reversible Monolayer Reorganization. In an STM experiment, changing current or bias voltage can cause perturbation

of an adsorbed phase, which can result in transformation to another, typically thermodynamically unstable, phase upon initial monolayer disruption.¹⁴ The outcome of this experiment for a two component monolayer, such as the 1D-cocrystal presented here, is not well preceded. In the present case, one part of the 1D-cocrystal changed to the phase of pure **17-*m*-diester** upon perturbation followed by a reversion to the 1D-cocrystal phase. Sequential STM images of this transformation from the **17-*m*-diester** phase to the 1D-cocrystal phase directly demonstrate the thermodynamic stability relationship. In an attempt to perturb the 1D-cocrystal (Figure 6a), the applied voltage was changed from 800 to 2000 mV and the monolayer scanned for 50 s. After this perturbation, designated $t = 0$, the applied voltage was returned to 800 mV to obtain the STM images in Figure 6. One area of the 1D-cocrystal was transformed to the pure **17-*m*-diester** phase (Figure 6b). After 100 s, the 1D-cocrystal phase is still changing to form the phase of **17-*m*-diester** (Figure 6c, white oval). This phase change results in the creation of a boundary area between **17-*m*-diester** and 1D-cocrystal phases. The molecularly resolved boundary area is indicated with the blue square in Figure 6c and additional boundary areas appear unresolved due to high mobility of molecules.^{14a} Because close packing is not satisfied in this area due to the mismatch of the two different phases (see Supporting Information), exchange of molecules occurs at the boundary area to build the thermodynamically more stable structure. If the hypothesis that filling the space near the adsorbed dimer with other dimers is thermodynamically more favorable than with a **17-*m*-diester** is correct, the boundary area should be transformed to a 1D-cocrystal phase by periodically inserting dimers of **18-amide**. This behavior was observed after 200 s through sequential STM images as evidenced by the **17-*m*-diester** starting to transform to the 1D-cocrystal phase by inserting dimers at the boundary area (Figure 6d). The broken 1D-cocrystal phase is recovering by periodically inserting dimers thus maintaining 1D periodicity (white oval circles in Figure 6d). This phenomenon proves that close packing is better satisfied by inserting the dimer of **18-amide** rather than **17-*m*-diester**. After 950 s, the **17-*m*-diester** phase is completely transformed to the initial 1D-cocrystal phase (Figure 6e, f). This result shows not only the formation process of the 1D-cocrystal but also demonstrates the potential of molecular switching using the physisorbed 1D-cocrystal on HOPG under ambient conditions.

2DSD Analysis. To put these results in the broader context of existing monolayers, a search of the Two-Dimensional Structural Database (2DSD) was conducted.¹⁵ The 2DSD construction and general molecular packing and symmetry of 2D crystals formed at the liquid/solid interface were previously reported.¹ This analysis revealed, for example, the close packing theory of 2D crystals is well supported by experimental data as evidenced by the frequency of certain plane groups. However, the types and frequency of the outcomes for crystallization from solutions containing two adsorbing species have not been reported in detail. These trends are analyzed here using the 2DSD and the present 1D-cocrystal is classified based on this analysis. Of the 876 entries in the 2DSD, 145 of these are formed from multicomponent solutions. Most frequently these are random mixtures (30.3%), but phase segregation (26.9%) and cocrystals (24.8%) are common and are distinct from the present 1D-cocrystal. Six cases of replacement (4.1%), which

(14) (a) Plass, K. E.; Matzger, A. J. *Chem. Commun.* **2006**, 3486. (b) Lu, X.; Polanyi, J. C.; Yang, J. *Nano Lett.* **2006**, *6*, 809–814.

(15) The 2DSD is now publicly available at <http://2dsd.lsa.umich.edu>.

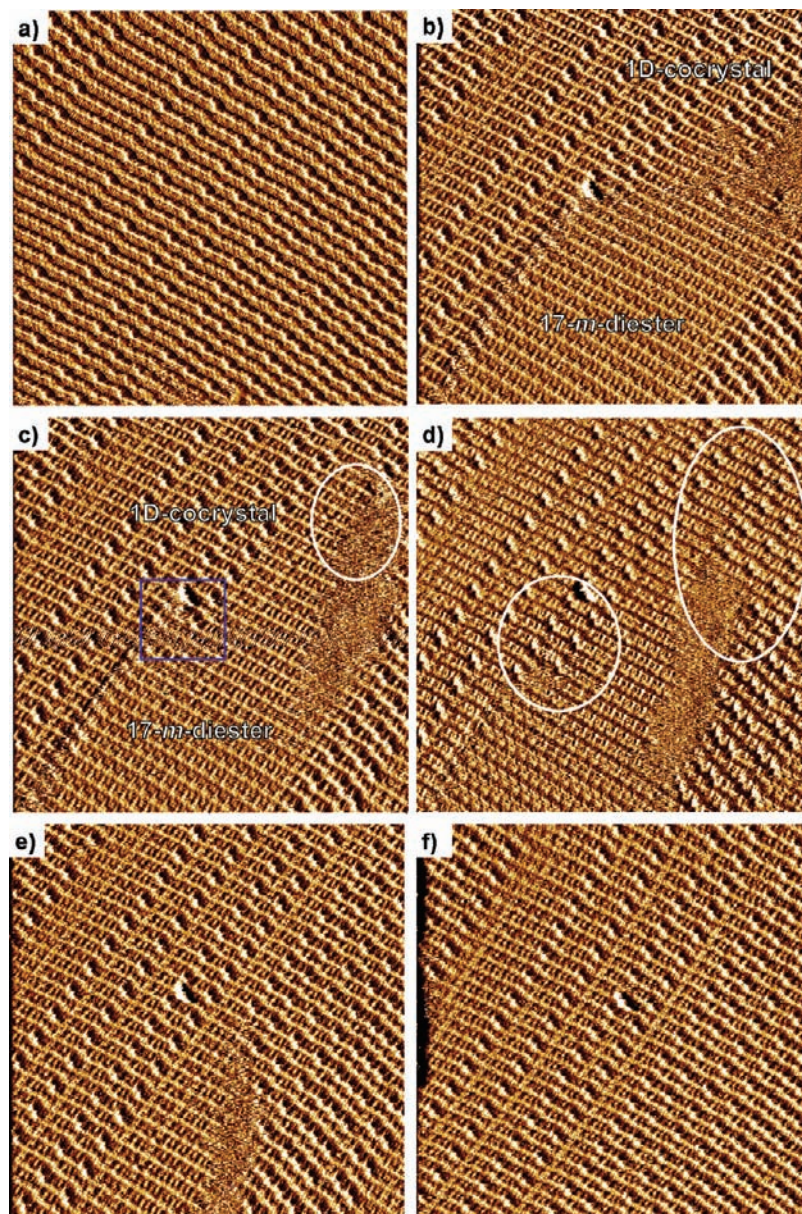


Figure 6. Sequential STM images from a 14:1 mixture (**17-*m*-diester**:**18-amide**) on HOPG ($80 \times 80 \text{ nm}^2$, 10.2 Hz, 800 mV, 300 pA). (a) 1D-Cocryystal (b) after applying 2000 mV for 50 s ($t = 0$) (c) 100 s (d) 200 s (e) 400 s (f) 950 s. A white oval indicates areas of significant change from the previous image and a blue square indicates the boundary area between **17-*m*-diester** and 1D-cocryystal phases.

is the phase change from the pure phase of one component to the pure phase of the other component, and nine cases of metal complexes (6.2%) are observed. Ten cases (6.9%) are not assigned because the paper reported the experiment but not the results or the image quality led to ambiguities in assignment. One case relating to the present 1D-cocryystal was found.¹⁶ An oligothiophene derivative containing side chain urea functionality inserted into the monourea derivative phase by forming hydrogen bonds between urea groups at one position in the bulk monolayer of the mono urea. Inserted oligothiophenes were oriented along one axis and an alignment shift of the monourea derivative phase to form another hydrogen bonding pattern was observed. However, there are two things different from the present case: (1) a uniform monolayer was not formed because

inserted oligothiophene molecules sometimes formed clusters of a few molecules and (2) an alignment shift occurred only once and an additional shift was not reported. By contrast, the average frequency of the alignment shift can be controlled through changing the molar ratio of components in the present case and complete coverage by a single phase is observed. The case of the oligothiophene derivative is consistent defect appearance at a domain boundary rather than a new type of periodic behavior. Therefore we regard the present 1D-cocryystal as a new type of 2D crystallization behavior to be considered as distinct from the commonly accepted outcomes of phase segregation, random mixing, and cocrySTALLIZATION.

Conclusion

X-ray diffraction, the most common method for studying structure of bulk crystalline materials, is poorly suited for studying materials with imperfect periodicity. The findings

(16) De Feyter, S.; Larsson, M.; Gesquiere, A.; Verheyen, H.; Louwet, F.; Groenendaal, B.; Esch, J.; Feringa, B. L.; De Schryver, F. *ChemPhysChem* **2002**, *11*, 966–969.

presented here demonstrate that the approach of using 2D crystallization monitored by STM as a model system for three-dimensional crystals offers mechanistic and structural insights not available using tools suited for studying three-dimensional crystals. During a competitive adsorption study, a novel type of coadsorption, 1D-cocrystal, distinguished from preceding outcomes from multicomponent solutions was observed. This assembly mode has characteristics of both random mixing and traditional stoichiometric cocrystallization and results in an alignment shift of the dominant phase. In addition, the frequency of the alignment shift can be controlled by variation of the ratio of adsorbates. This result demonstrates that the surface composition and patterns are variable through controlling the molar ratio of components and structural modulation is controlled perpendicular to the long molecular axis: the most difficult direction to control nanoprecision in these types of physisorbed monolayers. Identification of a new mode of assembly from multicomponent solutions is important due to the prevalence of

crystallization processes in purification and solid form engineering. Furthermore, because the observations were made on graphite, the findings are relevant to purification of materials by adsorption to carbonaceous sorbents containing graphitic domains.

Acknowledgment. This work was supported by the National Science Foundation (CHE-0616487).

Supporting Information Available: Experimental details, the model of the boundary area between **17-*m*-diester** and 1D-cocrystal phases, unit cell parameters and lattice energies of the periodic 1D-cocrystals, additional STM images of 1D-cocrystals and STM image of **17-*m*-diester** phase formed after the perturbation of 1D-cocrystal. This material is available free of charge via the Internet at <http://pubs.acs.org>.

JA905418U